JACS
JOURNAL OF THE AMERICAN CHEMICAL SOCIETY
Communication
pubs.acs.org/JACS

$BiFSeO_3$: An Excellent SHG Material Designed by Aliovalent Substitution

Ming-Li Liang,[†,‡] Chun-Li Hu,[†] Fang Kong,[*,†] and Jiang-Gao Mao[*,†]

[†]State Key Laboratory of Structural Chemistry, Fujian Institute of Research on the Structure of Matter, Chinese Academy of Sciences, Fuzhou 350002, P. R. China

[‡]College of Chemistry, Fuzhou University, Fuzhou 350108, P. R. China

Supporting Information

ABSTRACT: The first bismuth selenite fluoride, $BiFSeO_3$, was obtained by aliovalent substitution of 2D $BiOIO_3$. Its structure features a 3D network composed of 1D $[BiF]^{2+}$ chains interconnected by SeO_3 groups. $BiFSeO_3$ exhibits a very strong second harmonic generation (SHG) effect of about 13.5 times that of KH_2PO_4 (KDP) under 1064 nm laser radiation and 1.1 times that of $KTiOPO_4$ (KTP) under 2.05 μm laser radiation, which is the highest among all of the metal selenites reported. It has also very simple chemical composition and can be synthesized easily under mild hydrothermal conditions.

The exploration of new polar materials with strong second harmonic generation (SHG) has attracted great academic interest because a larger nonlinear coefficient usually means higher frequency conversion efficiency, which is crucial in nonlinear optical (NLO) materials.[1−3] Although many new NLO crystals have been discovered during the past two decades, it is still a great challenge to create novel compounds with large NLO effects.[4−6] Among these materials, metal selenites, tellurites, and iodates, which contain cations with lone pairs susceptible to second-order Jahn−Teller (SOJT) distortion, are very promising.[7−14] Generally, metal iodates and tellurites exhibit larger SHG effects than the corresponding metal selenites as a result of the larger polarizations of I−O and Te−O bonds compared with Se−O bonds.[7−14] To achieve higher SHG response, distorted octahedrally coordinated transition metal cations with a d^0 electronic configuration have been introduced into the above systems, leading to the discovery of many good SHG materials, including $Na_2Te_3Mo_3O_{16}$ (500 × α-SiO_2), $BaTeMo_2O_9$ (600 × α-SiO_2), $Li_2Ti(IO_3)_6$ (500 × α-SiO_2), and $BaNbO(IO_3)_5$ (14 × KH_2PO_4 (KDP)).[7−14] As for the metal selenites, the best SHG materials reported to date are $A_2(MoO_3)_3(SeO_3)$ (A = Tl, NH_4) (400 × α-SiO_2) and $Pb_2TiOF(SeO_3)_2Cl$ (9.6 × KDP).[10−14] However, these materials have complex chemical compositions, making their large-scale preparation and bulk single-crystal growth rather difficult tasks.

Recently it was shown that aliovalent substitution of d^0-TMO_6 octahedra in the above metal selenite systems can greatly enhance their SHG effects.[12,13] With the replacement of NbO_6 by TiO_5F, the SHG efficiency of $Pb_2Ti^{IV}OF(SeO_3)_2Cl$ is much larger than that of $Pb_2Nb^{V}O_2(SeO_3)_2Cl$ (2.3 × KDP).[12] In a similar way, we have dramatically increased the SHG effect of class-I hexagonal tungsten oxide-type materials from about 1 × KDP for $Cs(VO_2)_3(SeO_3)_2$ to 5 × KDP for $Cs(TiOF)_3(SeO_3)_2$ by the aliovalent substitution of $V^{V}O_6$ with $Ti^{IV}O_5F$.[13,14] This prompted us to think about whether we could design selenite-based high-performance SHG materials by the aliovalent substitution of polar metal iodates with large SHG responses and containing additional oxo anions: substitution of iodate groups by selenite groups and oxo anions by fluoride or hydroxide anions. Such metal selenites may be able to maintain a similar topology as the parent metal iodates, which have properly aligned polar units.[15] Furthermore, these materials would have very simple chemical compositions, and hence, their bulk sample preparation and large single-crystal growth would be relatively simple. On the basis of this idea, $BiOIO_3$ with a strong SHG efficiency (12.5 times that of KDP) was chosen as the parent compound.[16] Substitutions of iodate and oxo anions by selenite and fluoride anions, respectively, led to the discovery of $BiFSeO_3$ which exhibits a very large SHG response of about 13.5 times that of KDP and was synthesized under facile hydrothermal conditions. Herein we report its synthesis, crystal structure, and optical properties.

Single crystals of $BiFSeO_3$ were synthesized under hydrothermal conditions with a mixture of Bi_2O_3, SeO_2, and 40% HF solution in H_2O at 220 °C for 5 days (Figure 1). Energy-dispersive X-ray spectroscopy (EDS) analysis of several single crystals of $BiFSeO_3$ gave an average Bi/Se molar ratio of 1.0/1.1, which is very close to that determined from single-crystal

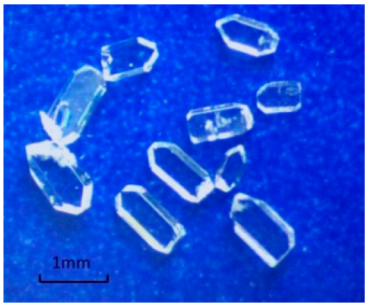

Figure 1. Image of the as-grown single crystals of $BiFSeO_3$.

Received: June 28, 2016
Published: July 18, 2016

DOI: 10.1021/jacs.6b06680
J. Am. Chem. Soc. 2016, 138, 9433−9436

X-ray structural analyses. Conspicuous peaks due to F appeared in the EDS spectrum. The measured powder X-ray diffraction (PXRD) pattern of $BiFSeO_3$ matched the simulation of its single-crystal data well (Figure S1), confirming the purity of the sample.

$BiFSeO_3$ crystallized in the same polar space group as $BiOIO_3$, namely, $Pca2_1$ (No. 29). Unlike the layered $BiOIO_3$, $BiFSeO_3$ features a three-dimensional (3D) framework composed of 1D $[BiF]^{2+}$ cationic chains further bridged by selenite anions (Figure 2a). The asymmetric unit of $BiFSeO_3$

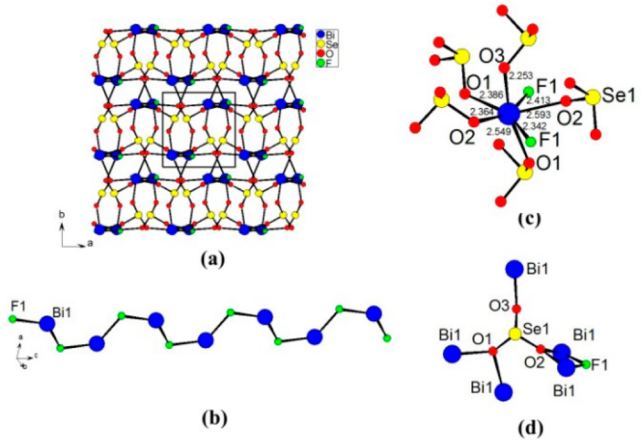

Figure 2. Views of (a) the structure of $BiFSeO_3$ along the *c* axis, (b) a 1D $[BiF]^{2+}$ chain along the *c* axis, (c) the coordination geometry around the Bi^{3+} cation, and (d) the coordination mode of the selenite anion.

contains one Bi^{3+} cation, one F^- anion, and one selenite anion. The seven-coordinate Bi(1) atom is bonded by five oxygen atoms from five selenite anions and two fluoride anions. Its coordination geometry can be best described as a severely distorted pentagonal bipyramid (Figure 2c). The Bi−O and Bi−F bond distances fall in the ranges of 2.253(8)−2.593(11) Å and 2.342(10)−2.413(12) Å, respectively, which are close to those reported in related compounds.[17] The Se^{4+} cation is a ψ-SeO_3 tetrahedron with one vertex occupied by a lone pair of electrons. The Se−O bond lengths are in the range of 1.689(16)−1.738(11) Å (Table S2). Bond valence calculations gave values of 2.82, 3.91, −0.71, and −1.95 to −2.04 for Bi(1), Se(1), F(1), and O(1)−O(3), respectively, indicating that they are in oxidation states of 3+, 4+, 1−, and 2−.[18]

The Bi^{3+} cations are interconnected by fluoride anions into 1D zigzag chains along the *c* axis (Figure 2b), and neighboring bismuth fluoride chains are further interconnected by bridging selenite anions to form a complex 3D network (Figure 2a). Each selenite anion is pentadentate and connects with five Bi atoms from four different bismuth fluoride chains (Figure 2d).

It is interesting to compare the structure of $BiFSeO_3$ with that of $BiOIO_3$ (Figure S2).[16] The structure of $BiOIO_3$ consists of $(Bi_2O_2)^{2+}$ cationic layers that are connected to IO_3^- anions. In both compounds, the lone pairs of selenite or iodate groups are aligned along the *c* axis, which is helpful for producing a large SHG response. Each oxo anion in $BiOIO_3$ is tetradentate and connects with four Bi atoms to form a $(Bi_2O_2)^{2+}$ cationic layer, and each iodate anion is tridentate and bridges three Bi atoms from the same $(Bi_2O_2)^{2+}$ cationic layer. Hence, the iodate groups hang above and below the $(Bi_2O_2)^{2+}$ cationic layer, producing a layered structure for the compound, and its *b* axis (11.0386 Å) is much larger than that of $BiFSeO_3$ (6.8872 Å), where the selenite groups act as linkers between neighboring $[BiF]^{2+}$ chains. These structural differences are due to the different sizes and coordination modes of the anions.

Thermogravimetric analysis (TGA) showed that this compound is stable up to 300 °C and then undergoes two main steps of weight loss, with a total weight loss of 35.8% in the temperature range of 300−820 °C (Figure S3), which corresponds to the release of SeO_2 and F_2. Differential scanning calorimetry (DSC) revealed two exothermic peaks at 456.5 and 834.6 °C, respectively. The F_2 released was detected by TGA−mass spectrometry (TG-MS) (Figure S4). The final residual at 850 °C was confirmed by PXRD to be mainly $BiO_{1.18}F_{0.64}$ (Figure S5).

The UV−vis−NIR diffuse-reflectance spectrum reveals that this compound is nearly transparent in the range of 2500−450 nm (Figure S6). The optical diffuse-reflectance spectrum measurements indicate that the optical band gap is approximately 3.83 eV for $BiFSeO_3$, which is blue-shifted compared with $BiOIO_3$ (3.3 eV).[16] $BiFSeO_3$ shows strong IR vibrational bands at 809.6, 684.2, and 643.6 cm^{-1}, which can be attributed to the characteristic absorption of the SeO_3^{2-} anion, and the peaks around 483.7 and 422.5 cm^{-1} can be assigned as Bi−O/F vibrations (Figure S7).

Powder SHG measurements revealed that the sample of $BiFSeO_3$ displays very strong signals in the visible and near-IR windows, and their SHG efficiencies are about 13.5 times that of KDP and 1.1 times that of $KTiPO_4$ (KTP) (Figure 3).

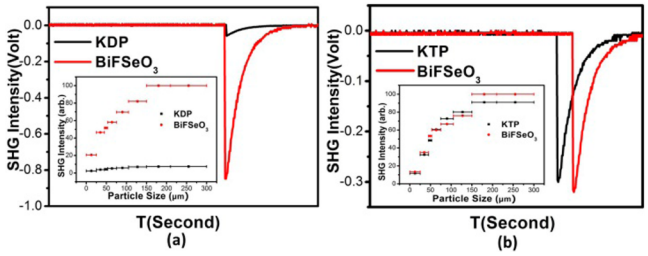

Figure 3. Oscilloscope traces of the SHG signals of $BiFSeO_3$ at (a) 1064 nm and (b) 2.05 μm. Plots of SHG intensity vs particle size are shown in the insets. KDP and KTP samples serve as the references at 1064 nm and 2.05 μm, respectively.

Furthermore, $BiFSeO_3$ is phase-matchable in both the visible and near-IR wavelength ranges. As far as we know, $BiFSeO_3$ exhibits the largest SHG response among all of the metal selenites reported.[10−14]

The SHG efficiency of $BiFSeO_3$ compares well to that of $BiOIO_3$ (12.5 × KDP), which may be ascribed to (1) the similar arrangements of the lone pairs of the SeO_3 groups in $BiFSeO_3$ and those of the IO_3 groups in $BiOIO_3$ and (2) the strengthened interlayer bonding for the 3D framework of $BiFSeO_3$ compared with the 2D framework of $BiOIO_3$. Usually, 3D structures are more beneficial to SHG applications than 2D structures, which can exhibit a strong layering crystal growth habit.[19]

To further study the underlying structure−property relationship for the NLO crystal $BiFSeO_3$, systematic theoretical calculations were performed using density functional theory. The calculated band structure (Figure S8) shows that $BiFSeO_3$ has an indirect band gap, and the calculated band gap is 3.65 eV, which is slightly lower than the experimental value (3.83 eV); hence, a scissor of 0.18 eV was applied in the calculations

DOI: 10.1021/jacs.6b06680
J. Am. Chem. Soc. 2016, 138, 9433−9436

of the optical properties of $BiFSeO_3$.[20] The partial density of states (PDOS) of $BiFSeO_3$ (Figure S9) reveals that the top of the valence band (VB) is dominated by O 2p nonbonding states and that the bottom of the conduction band (CB) mainly comes from empty Bi 6p and Se 4p orbitals. Therefore, the band gap of $BiFSeO_3$ is determined by Bi, Se, and O atoms.

On the basis of the space group ($Pca2_1$) and Kleinman symmetry, $BiFSeO_3$ has three independent SHG tensor components (d_{31}, d_{32}, and d_{33}). The absolute values of d_{31}, d_{32}, and d_{33} in the static limit are calculated to be 1.20×10^{-8}, 9.27×10^{-9}, and 7.99×10^{-9} esu, respectively. The results agree well with the experimentally measured powder SHG effect. Additionally, the calculated birefringence at 1064 nm (1.165 eV) is 0.144 (Figure S10), which is large enough to make the compound phase-matchable.

To investigate the origin of the strong SHG effect for $BiFSeO_3$, we performed further analysis of the largest tensor component, d_{31}. The spectral decomposition of d_{33} indicates that the energy regions on the two sides of the band gap (−2.3 to 0 eV in the VB and <4.8 eV in the CB) give the most positive contributions to the SHG effect, while the region of −4.9 to −2.3 eV contributes to the SHG effect negatively (bottom panel of Figure S9). Meanwhile, the SHG density of d_{31} was also calculated, allowing the orbital contribution to the SHG effect to be intuitively exhibited (Figure 4).[21] It can be

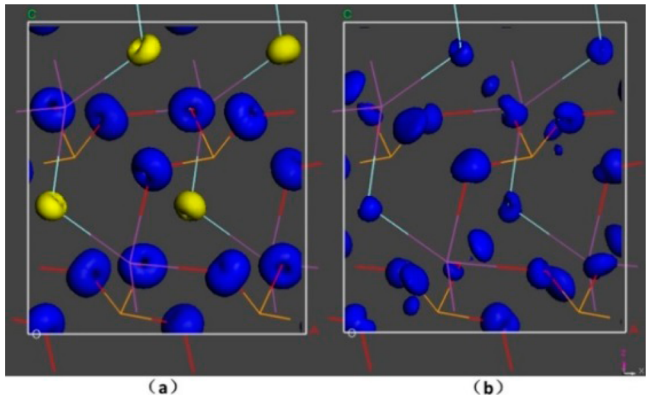

Figure 4. SHG density of d_{31} in (a) the valence band and (b) the conduction band of $BiFSeO_3$.

clearly observed that in the VB, the nonbonding 2p orbitals of all of the O atoms give the most contributions to the SHG, which is partly weakened by F 2p orbitals. In the CB, the SHG effect is mainly contributed by unoccupied Bi 6p and O 2p orbitals, mixing with some F 2p and Se 4p orbitals. Finally, we calculated all of the orbital contributions on the basis of the SHG density to obtain accurate contribution percentages of various groups. The results indicate that the contribution percentages of SeO_3 and BiO_5F_2 to d_{31} are 62.8% and 37.1%, respectively. We can conclude that the strong SHG response of $BiFSeO_3$ originates from the synergistic effect of SeO_3 and BiO_5F_2 groups.

In summary, the first 3D bismuth selenite fluoride, $BiFSeO_3$, was obtained by aliovalent substitution of a lone-pair cation (Se^{4+} for I^{5+}) and anion (F^- for O^{2-}) in layered $BiOIO_3$. Although the structure of $BiFSeO_3$ is 3D rather than 2D as in $BiOIO_3$, all of the selenite groups are aligned, similar to the iodate groups in $BiOIO_3$. The SHG efficiency of $BiFSeO_3$ is the highest among all metal selenites reported. The material is phase-matchable, and its chemical composition and its preparation method are rather simple. Hence, it could be a new promising SHG material. This study has provided a feasible approach to design new high-performance NLO materials.

■ ASSOCIATED CONTENT

Supporting Information

The Supporting Information is available free of charge on the ACS Publications website at DOI: 10.1021/jacs.6b06680.

Detailed synthesis description, crystal structure determination, theoretical calculations, TG−MS data, and IR and UV−vis spectra (PDF)

Crystallographic data for $BiFSeO_3$ (CIF)

■ AUTHOR INFORMATION

Corresponding Authors

*kongfang@fjirsm.ac.cn

*mjg@fjirsm.ac.cn

Notes

The authors declare no competing financial interest.

■ ACKNOWLEDGMENTS

This work was supported by the National Natural Science Foundation of China (Grants 91222108, 21373222, and 21231006), the CAS Youth Innovation Promotion Association, and the Strategic Priority Research Program of the Chinese Academy of Sciences (Grant XDB20000000).

■ REFERENCES

(1) (a) Wickleder, M. S. *Chem. Rev.* **2002**, *102*, 2011. (b) Ok, K. M.; Chi, E. O.; Halasyamani, P. S. *Chem. Soc. Rev.* **2006**, *35*, 710.

(2) Zhang, W.; Xiong, R. G. *Chem. Rev.* **2012**, *112*, 1163.

(3) Hu, C. L.; Mao, J. G. *Coord. Chem. Rev.* **2015**, *288*, 1.

(4) (a) Pan, S. L.; Smit, J. P.; Watkins, B.; Marvel, M. R.; Stern, C. L.; Poeppelmeier, K. R. *J. Am. Chem. Soc.* **2006**, *128*, 11631. (b) Lu, H. C.; Gautier, R.; Donakowski, M. D.; Tran, T. T.; Edwards, B. W.; Nino, J. C.; Halasyamani, P. S.; Liu, Z. T.; Poeppelmeier, K. R. *J. Am. Chem. Soc.* **2013**, *135*, 11942. (c) Dong, X. Y.; Jing, Q.; Shi, Y. J.; Yang, Z. H.; Pan, S. L.; Poeppelmeier, K. R.; Young, J.; Rondinelli, J. M. *J. Am. Chem. Soc.* **2015**, *137*, 9417. (d) Wu, H. P.; Yu, H. W.; Yang, Z. H.; Hou, X. L.; Su, X.; Pan, S. L.; Poeppelmeier, K. R.; Rondinelli, J. M. *J. Am. Chem. Soc.* **2013**, *135*, 4215.

(5) (a) Zou, G.; Huang, L.; Ye, N.; Lin, C.; Cheng, W.; Huang, H. *J. Am. Chem. Soc.* **2013**, *135*, 18560. (b) Wang, S. C.; Ye, N. *J. Am. Chem. Soc.* **2011**, *133*, 11458. (c) Yu, H. W.; Zhang, W. G.; Young, J.; Rondinelli, J. M.; Halasyamani, P. S. *J. Am. Chem. Soc.* **2016**, *138*, 88. (d) Wu, Q.; Liu, H. M.; Jiang, F. C.; Kang, L.; Yang, L.; Lin, Z. S.; Hu, Z. G.; Chen, X. G.; Meng, X. G.; Qin, J. G. *Chem. Mater.* **2016**, *28*, 1413.

(6) (a) Wang, S. A.; Alekseev, E. V.; Ling, J.; Liu, G. K.; Depmeier, W.; Albrecht-Schmitt, T. E. *Chem. Mater.* **2010**, *22*, 2155. (b) Wang, S. A.; Alekseev, E. V.; Diwu, J.; Miller, H. M.; Oliver, A. G.; Liu, G. K.; Depmeier, W.; Albrecht-Schmitt, T. E. *Chem. Mater.* **2011**, *23*, 2931.

(7) (a) Sun, C. F.; Hu, C. L.; Xu, X.; Yang, B. P.; Mao, J. G. *J. Am. Chem. Soc.* **2011**, *133*, 5561. (b) Sun, C. F.; Hu, C. L.; Xu, X.; Ling, J. B.; Hu, T.; Kong, F.; Long, X. F.; Mao, J. G. *J. Am. Chem. Soc.* **2009**, *131*, 9486. (c) Phanon, D.; Gautier-Luneau, I. *Angew. Chem., Int. Ed.* **2007**, *46*, 8488. (d) Chang, H. Y.; Kim, S. H.; Halasyamani, P. S.; Ok, K. M. *J. Am. Chem. Soc.* **2009**, *131*, 2426.

(8) (a) Goodey, J.; Broussard, J.; Halasyamani, P. S. *Chem. Mater.* **2002**, *14*, 3174. (b) Lee, D. W.; Ok, K. M. *Inorg. Chem.* **2013**, *52*, 6236. (c) Chi, E. O.; Ok, K. M.; Porter, Y.; Halasyamani, P. S. *Chem. Mater.* **2006**, *18*, 2070. (d) Ra, H. S.; Ok, K. M.; Halasyamani, P. S. *J. Am. Chem. Soc.* **2003**, *125*, 7764.

DOI: 10.1021/jacs.6b06680
J. Am. Chem. Soc. 2016, 138, 9433−9436

(9) (a) Zhang, J. J.; Zhang, Z. H.; Sun, Y. X.; Zhang, C. Q.; Zhang, S. G.; Liu, Y.; Tao, X. T. *J. Mater. Chem.* **2012**, *22*, 9921. (b) Zhang, J. J.; Zhang, Z. H.; Sun, Y. X.; Zhang, C. Q.; Tao, X. T. *CrystEngComm* **2011**, *13*, 6985. (c) Yu, D. H.; Sun, D. H.; Avdeev, M.; Wu, Q.; Tian, X. X.; Gu, Q. F.; Tao, X. T. *Cryst. Growth Des.* **2015**, *15*, 3110. (d) Feng, X. X.; Zhang, J. J.; Gao, Z. L.; Zhang, S. J.; Sun, Y. X.; Tao, X. T. *Appl. Phys. Lett.* **2014**, *104*, 081912.

(10) (a) Kong, F.; Huang, S. P.; Sun, Z. M.; Mao, J. G.; Cheng, W. D. *J. Am. Chem. Soc.* **2006**, *128*, 7750. (b) Johnston, M. G.; Harrison, W. T. A. *Eur. J. Inorg. Chem.* **2011**, *2011*, 2967. (c) Bang, S. E.; Lee, D. W.; Ok, K. M. *Inorg. Chem.* **2014**, *53*, 4756. (d) Geng, L.; Li, Q.; Meng, C. Y.; Dai, K.; Lu, H. Y.; Lin, C. S.; Cheng, W. D. *J. Mater. Chem. C* **2015**, *3*, 12290.

(11) (a) Chang, H. Y.; Kim, S. W.; Halasyamani, P. S. *Chem. Mater.* **2010**, *22*, 3241. (b) Harrison, W. T. A.; Dussack, L. L.; Vogt, T.; Jacobson, A. J. *J. Solid State Chem.* **1995**, *120*, 112. (c) Harrison, W. T. A.; Dussack, L. L.; Jacobson, A. J. *Inorg. Chem.* **1994**, *33*, 6043. (d) Kim, Y. H.; Lee, D. W.; Ok, K. M. *Inorg. Chem.* **2014**, *53*, 1250.

(12) Cao, X. L.; Hu, C. L.; Xu, X.; Kong, F.; Mao, J. G. *Chem. Commun.* **2013**, *49*, 9965.

(13) Cao, X. L.; Hu, C. L.; Kong, F.; Mao, J. G. *Inorg. Chem.* **2015**, *54*, 3875.

(14) (a) Harrison, W. T. A.; Buttery, J. H. N. *Z. Anorg. Allg. Chem.* **2000**, *626*, 867. (b) Vaughey, J. T.; Harrison, W. T. A.; Dussack, L. L.; Jacobson, A. J. *Inorg. Chem.* **1994**, *33*, 4370. (c) Harrison, W. T. A.; Dussack, L. L.; Jacobson, A. J. *Acta Crystallogr., Sect. C: Cryst. Struct. Commun.* **1995**, *51*, 2473.

(15) (a) Eaton, T.; Lin, J.; Cross, J. N.; Stritzinger, J. T.; Albrecht-Schmitt, T. E. *Chem. Commun.* **2014**, *50*, 3668. (b) Kong, F.; Xu, X.; Mao, J. G. *Inorg. Chem.* **2010**, *49*, 11573.

(16) Nguyen, S. D.; Yeon, J.; Kim, S. H.; Halasyamani, P. S. *J. Am. Chem. Soc.* **2011**, *133*, 12422.

(17) (a) Laval, J. P.; Champarnaud-Mesjard, J. C.; Britel, A.; Mikou, A. *J. Solid State Chem.* **1999**, *146*, 51. (b) Cong, R. H.; Wang, Y.; Kang, L.; Zhou, Z. Y.; Lin, Z. S.; Yang, T. *Inorg. Chem. Front.* **2015**, *2*, 170.

(18) (a) Brese, N. E.; O'Keeffe, M. *Acta Crystallogr., Sect. B: Struct. Sci.* **1991**, *47*, 192. (b) Brown, I. D.; Altermatt, D. *Acta Crystallogr., Sect. B: Struct. Sci.* **1985**, *41*, 244.

(19) (a) Chen, C. T.; Wang, G. L.; Wang, X. Y.; Xu, Z. Y. *Appl. Phys. B: Lasers Opt.* **2009**, *97*, 9. (b) Zhao, S. G.; Zhang, J.; Zhang, S. Q.; Sun, Z. H.; Lin, Z. S.; Wu, Y. C.; Hong, M. C.; Luo, J. H. *Inorg. Chem.* **2014**, *53*, 2521. (c) Yu, H. W.; Wu, H. P.; Pan, S. L.; Yang, Z. H.; Hou, X. L.; Su, X.; Jing, Q.; Poeppelmeier, K. R.; Rondinelli, J. M. *J. Am. Chem. Soc.* **2014**, *136*, 1264. (d) Kang, L.; Luo, S. Y.; Peng, G.; Ye, N.; Wu, Y. C.; Chen, C. T.; Lin, Z. S. *Inorg. Chem.* **2015**, *54*, 10533.

(20) (a) Godby, R. W.; Schluter, M.; Sham, L. J. *Phys. Rev. B: Condens. Matter Mater. Phys.* **1987**, *36*, 6497. (b) Okoye, C. M. I. *J. Phys.: Condens. Matter* **2003**, *15*, 5945. (c) Terki, R.; Bertrand, G.; Aourag, H. *Microelectron. Eng.* **2005**, *81*, 514.

(21) (a) Xu, X.; Hu, C. L.; Li, B. X.; Yang, B. P.; Mao, J. G. *Chem. Mater.* **2014**, *26*, 3219. (b) Song, J.-L.; Hu, C.-L.; Xu, X.; Kong, F.; Mao, J.-G. *Angew. Chem., Int. Ed.* **2015**, *54*, 3679.

DOI: 10.1021/jacs.6b06680
J. Am. Chem. Soc. 2016, 138, 9433−9436